ASTROBIOLOGY
Volume 2, Number 4, 2002


# Research Paper

# Long-Term Manipulations of Intact Microbial Mat Communities in a Greenhouse Collaboratory: Simulating Earth's Present and Past Field Environments

BRAD M. BEBOUT,[1] STEVEN P. CARPENTER,[1] DAVID J. DES MARAIS,[1] MYKELL DISCIPULO,[2] TSEGEREDA EMBAYE,[2] FERRAN GARCIA-PICHEL,[3] TORI M. HOEHLER,[1] MARY HOGAN,[4] LINDA L. JAHNKE,[1] RICHARD M. KELLER,[5] SCOTT R. MILLER,[6] LESLIE E. PRUFERT-BEBOUT,[1] CHRIS RALEIGH,[7] MICHAEL ROTHROCK,[3] and KENDRA TURK[4]

## ABSTRACT

**Photosynthetic microbial mat communities were obtained from marine hypersaline saltern ponds, maintained in a greenhouse facility, and examined for the effects of salinity variations. Because these microbial mats are considered to be useful analogs of ancient marine communities, they offer insights about evolutionary events during the >3 billion year time interval wherein mats co-evolved with Earth's lithosphere and atmosphere. Although photosynthetic mats can be highly dynamic and exhibit extremely high activity, the mats in the present study have been maintained for >1 year with relatively minor changes. The major groups of microorganisms, as assayed using microscopic, genetic, and biomarker methodologies, are essentially the same as those in the original field samples. Field and greenhouse mats were similar with respect to rates of exchange of oxygen and dissolved inorganic carbon across the mat–water interface, both during the day and at night. Field and greenhouse mats exhibited similar rates of efflux of methane and hydrogen. Manipulations of salinity in the water overlying the mats produced changes in the community that strongly resemble those observed in the field. A collaboratory testbed and an array of automated features are being developed to support remote scientific experimentation with the assistance of intelligent software agents. This facility will permit teams of investigators the opportunity to explore ancient environmental conditions that are rare or absent today but that might have influenced the early evolution of these photosynthetic ecosystems. Key Words: Microbial mat—Biogeochemistry—Biomarkers. Astrobiology 2, 383–402.**

[1]Exobiology Branch and [5]Computational Sciences Division, NASA Ames Research Center, Moffett Field, California.
[2]SETI Institute, Mountain View, California.
[3]Department of Microbiology, Arizona State University, Tempe, Arizona.
[4]Institute of Marine Sciences, University of California, Santa Cruz, California.
[6]Department of Genetics, North Carolina State University, Raleigh, North Carolina.
[7]Montana State University, Bozeman, Montana.

## INTRODUCTION

Modern microbial mats are thought to be extant representatives of Earth's most ancient ecosystems (Walter, 1976). Geochemical evidence of the existence of photosynthetic microbial mats, and their mineralized counterparts, stromatolites, has been identified in rocks as old as 3.0 Ga (Beukes and Lowe, 1989). As a living repository of genetic, physiological, isotopic, and biogeochemical information on the co-evolution of a planet and the only known biosphere, modern microbial mats are invaluable objects of study. Modern microbial mat studies have provided important insights on rates of biological activity (Revsbech *et al.,* 1983; Canfield and Des Marais, 1993; Des Marais, 1995), genetic diversity (Ward *et al.,* 1990; Garcia-Pichel *et al.,* 1998; Nübel *et al.,* 2001), stable isotopic fractionation (Schidlowski, 1988; Des Marais and Canfield, 1994), and organic (Boon, 1984; Ward *et al.,* 1985) and atmospheric (Visscher and Van Gemerden, 1991; Visscher and Kiene, 1994; Hoehler *et al.,* 2001) biomarkers, as well as minerals (Reid *et al.,* 2000), that have been used to interpret the fossil record of these communities over geologic time.

Photosynthetic microbial mats are self-sustaining, complete ecosystems in which light energy absorbed over a diel (24-h) cycle drives the synthesis of spatially organized, diverse biomass. Microorganisms with tightly coupled metabolisms in the mat catalyze transformations of carbon, nitrogen, sulfur, and metals. Radiant energy from the sun sustains oxygenic and anoxygenic photosynthesis, which in turn provides chemical energy (as organic photosynthates and oxygen) to the rest of the community. When oxygenic photosynthesis ceases at night, the upper layers of the mat become highly reduced and sulfidic (Jørgensen *et al.,* 1979). Counteracting gradients of oxygen and sulfide shape the chemical environment and provide daily-contrasting microenvironments separated on a scale of a few millimeters (Revsbech *et al.,* 1983; Revsbech and Jørgensen, 1986). While photosynthetic bacteria dominate the biomass and productivity of the mat, many aspects of the ecosystem's emergent behavior may ultimately depend on the associated nonphotosynthetic microbial communities, including the anaerobes. Additionally, transformation of photosynthetic productivity by the microbial community may contribute diagnostic "biosignature" gases that could represent search targets for remote spectroscopic life detection efforts [e.g., Terrestrial Planet Finder (Des Marais *et al.,* 2002)]. To understand the overall structure and function of mat communities, it is thus critical to determine the nature and extent of the interactions between phototrophic and nonphotosynthetic microorganisms, including anaerobic microorganisms.

Compared with their historical distribution and abundance, microbial mats are today confined to a relatively restricted number of habitats. Well-developed modern photosynthetic mats occur in both high-salinity and high-temperature environments. This restricted distribution is thought to be due primarily to the higher rates of grazing in more moderate modern environments (Garret, 1970), although alternative hypotheses have been forwarded. In any event, the limited geographical distribution of mats on the present-day Earth also serves to limit their usefulness as analogs of similar ecosystems growing in more diverse ancient environments. Environments that are not well represented on the modern Earth, but that have been extremely important over evolutionary time, include marine environments having low concentrations of sulfate and/or free oxygen (Holland, 1984; Canfield and Teske, 1996).

The effects on microbial processes of various environmental parameters important in Earth's past (such as sulfate and oxygen concentrations) may be studied in culture. However, the emergent properties of complex microbial ecosystems are not necessarily predictable, or understandable, on the basis of these types of experiments (Wilson and Botkin, 1990). Either some microbial processes do not occur in culture [e.g., anaerobic methane oxidation (Reeburgh, 1980) and sulfate reduction under aerobic conditions (Canfield and Des Marais, 1991)], or they occur at rates vastly different than rates observed in nature. In addition, relatively few (<1%) of the total number of microbes present in nature are available in culture (Ward *et al.,* 1990; Amann *et al.,* 1995). A microbial mat is a highly complex assemblage of organisms possessing many different modes of metabolism, all of which are interacting with each other at some level in beneficial and/or competitive ways. The end products of the metabolism of one group of organisms frequently constitute the substrates of another. These considerations argue for an alternative approach in which the entire microbial ecosystem is subjected to experimental manipulation.

To attain several key objectives in astrobiology, we must understand better the mechanisms and rates at which trace gases are produced and consumed by microbial ecosystems. As dominant components of our biosphere for at least 2 billion years of its >3.5 billion year history, microbial mats played a pivotal role in shaping the composition of Earth's early atmosphere, including its eventual oxygenation. NASA's present search strategy for the detection of life on extrasolar planets includes the observation and interpretation of spectral features of biogenic gases in remote atmospheres (Des Marais *et al.*, 2002). However, the current strategy relies principally upon the detection of $O_2$, and thus might preclude the detection of life that might resemble our own pre-oxygenated biosphere for as much as 2 billion years of its early existence. Clearly, the rates of production and consumption of reduced gases by microbial communities over geologic time must be better constrained to enhance our search for life elsewhere. The use of simulation facilities, such as the greenhouse described here, will augment that endeavor.

We report here our attempts to maintain intact modern photosynthetic microbial mats under approximate *in situ* conditions, and to monitor the responses of these mats to experimental manipulations. We have constructed a facility in which photosynthetic microbial mats can be maintained over long periods of time, using natural illumination and realistic water flow and other environmental conditions. We describe here the results of our first experiment, in which we used this facility to manipulate the salinity of water overlying the mats. As variations in salinity also occur in the natural environment where these mats were collected, we are able to assess the degree to which our experimental facility can reproduce naturally occurring phenomena. Future uses of this experimental system, in which conditions not presently found in the modern environment will be simulated, are discussed.

## MATERIALS AND METHODS

### *Field site*

Microbial mats were collected in salterns managed by the salt-producing company Exportadora de Sal. S.A. de C.V., located on the Pacific Ocean side of the Peninsula of Baja California Sur, Mexico. This field site was previously described in detail (Des Marais, 1995). Briefly, lagoon water, having a salinity of ~40‰ (parts per thousand), is pumped through a series of concentrating ponds, and then into crystallizing ponds. The salinity of the water is gradually raised until it becomes saturated with respect to sodium chloride, at which point the brine is pumped out of the crystallizing pond, and the salt is harvested. Extensive and well-developed microbial mats occur in concentrating areas in which the salinity is between ~65‰ and 130‰.

Microbial mats were collected on May 27, 2000 from two localities: Area 4, near the dike separating Area 4 from Area 5 (27°41.3450′N, 113°55.0270′W), and Area 5, near the dike separating Area 5 from Area 6 (27°44.4140′N, 113°54.7950′W). At the time of the collection, the salinities of Area 4 and Area 5 were ~90‰ and ~120‰, respectively. Microbial mats in both of these locations are ~5 cm thick and well laminated. The dominant cyanobacterium of the mat community is *Microcoleus chthonoplastes*. Sections of mat ~20 × 25 cm were cut and removed from the bottom of the concentrating pond by divers using metal spatulas and were immediately placed into tight-fitting black acrylic trays. In this way, exposure of the deeper anaerobic layers of the mats to air and light was minimized. Mats were covered with relatively high-salinity water (180‰) overnight in an effort to slow overall metabolic rates for transport. The trays containing the mats were then transported by vans back to our laboratory in larger plastic trays covered by tight-fitting plastic film. In this way, the mats were kept moist but not covered with water, and were exposed to some natural light over the ~48 h required for the relocation. Although six mats from Area 5 and 12 mats from Area 4 were maintained in the greenhouse throughout the entire experiment, results from only the Area 4 mats will be presented here.

### *Greenhouse facility*

Upon arrival at Ames Research Center, the mats were transferred to a greenhouse modified for these experiments by replacing the original glass with UV-transparent OP-4 acrylic (transmission in the UV-B, UV-A, and visible ~90% in the greenhouse). Mats were placed onto a specially built table (Fig. 1) having six clear acrylic flow boxes (150 × 22 cm), each flow box holding

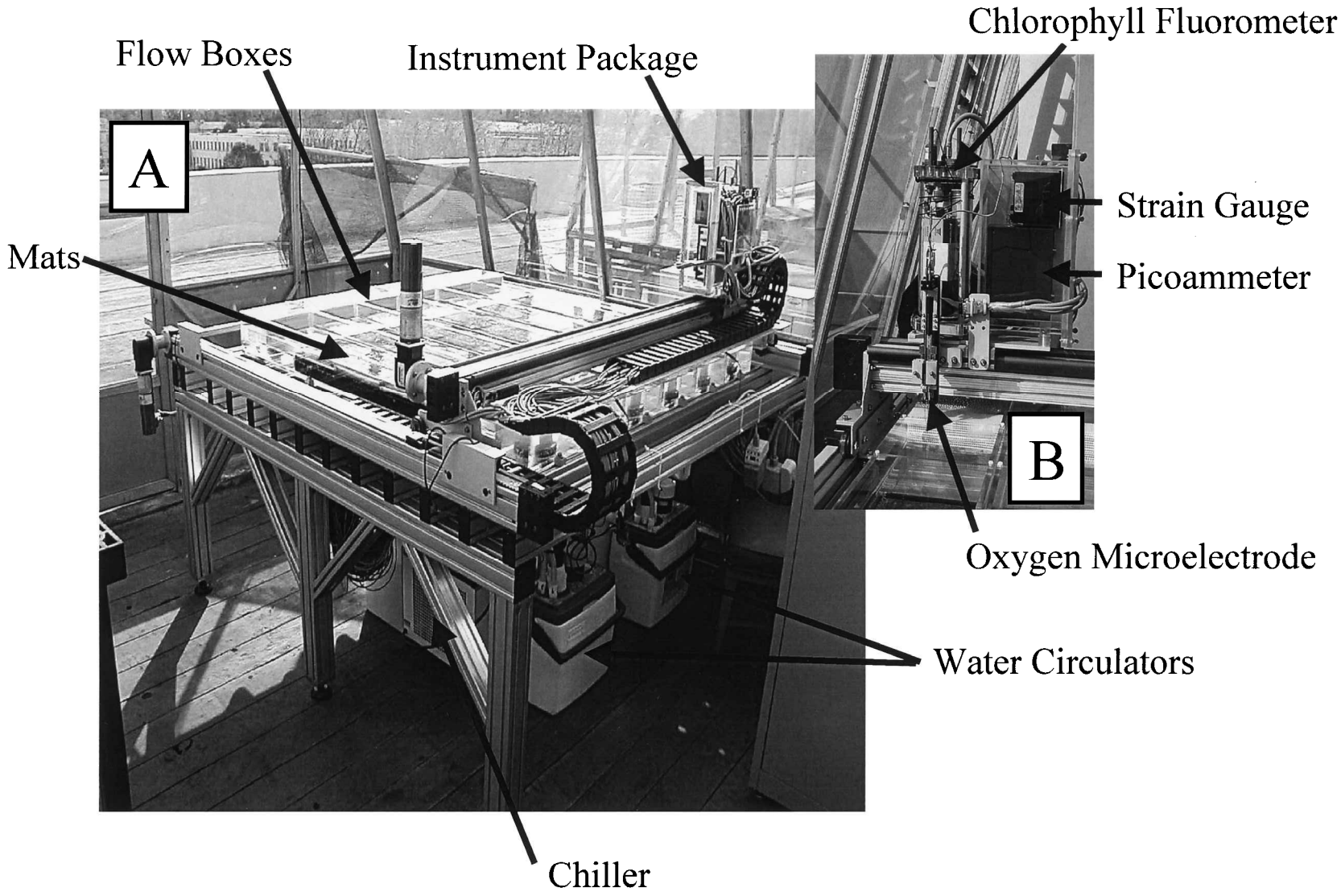


**FIG. 1. Microbial mats positioned on the table used in the latter half of the experiment.** Three mats are incubated in each of the six acrylic flow boxes. The positions of the reservoirs and temperature control equipment can be seen (**B**), as well as the instrument package (**A**) present on the remotely operable *xyz* table. Photo credit: Dan Andrews.

three trays of mat. The depth of the water in the flow boxes can be adjusted with standpipes. For this experiment, the depth of the water overlying the mats was ~3 cm; therefore the total volume of the water in each flow box at any one time was ~10 L.

Brine used for the experiment was collected from one of the higher-salinity (~130‰) concentrating areas that had retained its original complement of seawater solutes, and diluted with deionized water to the appropriate salinity. Mats were arbitrarily assigned to one of two salinity treatments on the table. Three of the flow boxes recirculated brine collected from the field site, which was diluted to the *in situ* salinity of 90‰ (hereafter referred to as the NORMAL salinity treatment). The other three flow boxes recirculated brine having an elevated salinity of 120‰ (hereafter referred to as the HIGH salinity treatment). Water was recirculated from a single reservoir holding 60 L of brine through the three interconnected flow boxes that constituted each of the two salinity treatments.

### *Environmental control*

The flow boxes assigned to each of the salinity treatments were interspersed on the table, so that the treatments alternated (e.g., NORMAL, HIGH, NORMAL, etc.). Salinity was maintained at these levels over the course of the experiment with additions of deionized water to replace losses due to evaporation. Temperature control of the air in the greenhouse was achieved with a combination of an evaporative cooler and propane heater. Precise temperature control of the water being recirculated over the mats was achieved by circulating temperature-controlled water through titanium heat-exchanging coils submerged in the reservoirs. Normal *in situ* daily water column temperature variations were simulated in the greenhouse by (1) controlling the temperature increase (attributable to solar heating) during the daytime to stay below the maximum temperature observed *in situ* and (2) turning off temperature control at night to allow the water temperature in the flow boxes to decrease slowly with the decrease in greenhouse air temperature. This simulation of diel temperature variations, while not always completely faithful to the precise near-sinusoidal pattern of temperature change observed *in situ* (owing to the simplicity of the apparatus), reproduced the normal range of temperatures observed *in situ* and the approximate duration of time at each temperature. The similarity between greenhouse and *in situ* temperatures was documented by an extensive set of measurements performed the year after this experiment was run. However, since no changes had been made to the apparatus since the time of the experiments reported here, this comparison should be valid for the period of time discussed here. Using submersible data loggers (StowAway TidbiT, Onset Computer Corp., Bourne, MA), recording at 10-min intervals from June 2001 through September 2001, the average temperature in the salterns was $22.8 \pm 1.99$°C (mean ± SD, for $n = 16{,}914$), whereas water temperatures in the greenhouse over the same interval of time were $20.3 \pm 2.62$°C ($n = 16{,}191$). Water column salinity in the flow boxes was determined using a refractometer (Delta model, Bellingham + Stanley, Tunbridge Wells, UK), which was corrected for temperature effects at each reading. Light [as photosynthetically available radiation (PAR)] was monitored and averaged at 10-min intervals, using a data logger coupled to a terrestrial quantum sensor (LI-1000 and LI-192SA, LI-COR, Inc., Lincoln, NE). An underwater light sensor (LI 192SA, LI-COR, Inc.) was used to measure irradiance at the mat surface *in situ* on several field trips. The irradiance at the mat surface, expressed as a percentage of the irradiance incident upon the surface of the pond, is comparable with measurements of irradiance in the greenhouse.

### *Greenhouse oxygen microelectrode measurements*

Oxygen concentrations within the microbial mats were monitored at various times throughout the course of the experiment using oxygen microelectrodes. We used Clark-type microelectrodes incorporating guard cathodes (model 737-GC, Diamond General Development Corp., Ann Arbor, MI). In the initial phase of the experiment, microelectrodes were positioned using motorized micromaniupulators mounted to bases placed across the flow boxes. Halfway through the experiment, the microsensors were transitioned to a positioning system using a robotic *xyz* positioning system installed over the flow boxes (Fig. 1). In all cases, the positioning was controlled by, and data were acquired with, custom software written in the LabVIEW programming environment (National Instruments Corp., Austin, TX).

In general, the electrodes were advanced

within the mat at 100-$\mu$m steps. Oxygen microelectrode signal output was calibrated to oxygen concentrations using a two-point calibration. Because the water circulating through the flow boxes was constantly aerated through the action of the pumps and through contact with the atmosphere across a large surface area of water, the electrode current at any point in the water overlying the mats was taken to be equal to the current produced in air-saturated water at that particular temperature and salinity. The exact value of this oxygen concentration can then be identified using published values (Sherwood *et al.,* 1991). The second point in the calibration, the output of the electrode at an oxygen concentration of 0, was provided by the asymptotic minimum of electrode current within the permanently anoxic lower parts of the mat.

### In situ *microelectrode measurements*

Measurements of *in situ* concentrations of oxygen within the microbial mat were made using a diver-operated microprofiler (Unisense, Århus, Denmark) at 100-$\mu$m intervals. Calibrations of the oxygen electrode were performed as described for greenhouse microelectrodes (above). As the ponds are well mixed during windy periods of the day, electrode readings in the well-mixed portions of the water column above the mat surface were taken to represent air-saturated values at a given temperature and salinity. In the morning, bottom water can be low in oxygen and, therefore, was not used for electrode calibrations; rather, readings closer to the air–water interface were used to calibrate the electrodes. In all cases, measurements of the asymptotic minimum in electrode current within the permanently anoxic lower parts of the mat were used as the zero oxygen concentration calibration point.

### *Community composition analyses*

*Light microscopy.* Microbial community composition was followed throughout the course of the experiment using a variety of techniques. First-order observations about the community were made using light microscopy (Nikon Microphot FX/A, Nikon USA). We did not employ quantitative microscopy techniques, and so these observations will be referred to as "nonquantitative" microscope observations.

*Cyanobacterial 16S rRNA gene fingerprints by polymerase chain reaction (PCR)/denaturing gradient gel electrophoresis (DGGE).* Cores (10 mm in diameter) were taken from the microbial mats on September 15, 2000, and the photic zone (top 3 mm) was aseptically removed. The samples were homogenized in a Tenbroeck tissue grinder (VWR Scientific Products, Brisbane, CA). Cell lysis and DNA extraction were performed as previously described (Nübel *et al.,* 1997). In short, the homogenized samples were frozen and thawed repeatedly, followed by incubation with 1% sodium dodecyl sulfate and proteinase K. DNA extraction was performed using hexadecylmethylammonium bromide in conjunction with phenol/chloroform/isoamyl alcohol (25:24:1 by volume), followed by isopropyl alcohol precipitation. Cyanobacterial/plastid-specific PCR amplification was carried out using the oligonucleotide primers CYA359F (with a 40-nucleotide GC-rich sequence at the 5′ end) and CYA805R, which were used for specific amplification of 16S rRNA genes from cyanobacteria and plastids (Nübel *et al.,* 1997). Each 50-$\mu$L PCR mixture contained 5 $\mu$L of 10× Takara Ex Taq™ PCR buffer (PanVera Corp., Madison, WI), 4 $\mu$L of Takara deoxynucleotide triphosphate mixture (2.5 m*M* each), 50 pmol of each primer, 200 $\mu$g of bovine serum albumin, 10 $\mu$L of 5× Eppendorf TaqMaster™ PCR-enhancer (Brinkmann Instruments, Inc., Westbury, NY), and 15 ng of DNA extract. Thermocycling was performed using a Bio-Rad iCycler™ thermal cycler (Bio-Rad Laboratories, Hercules, CA). After an initial denaturation at 94°C for 5 min (hot start), 2.5 units of Takara Ex Taq DNA polymerase was added to the reaction at 80°C. Thirty-five cycles of 1 min each at 94°C (denaturation), 60°C (annealing), and 72°C (extension) were performed, and the reaction finished with a final extension at 72°C for 9 min. Gels were imaged using a Bio-Rad Fluor-S™ MultiImager system. For DGGE band sequencing, each band was excised using a sterile scalpel, and DNA was allowed to diffuse out for ≥3 days at 4°C in 50 $\mu$L of 10 m*M* Tris buffer. One microliter of the solution was PCR-amplified using the same primers, reaction mixture, and thermocycling conditions. A kit was used to purify PCR product (Qiagen, Inc., Valencia, CA) and 150 ng was commercially sequenced in two separate reactions (5′ to 3′ and 3′ to 5′). Complementary sequences were matched, aligned, and edited using Sequence Navigator (Applied Biosystems, Foster

City, CA) and submitted to the BLAST search engine (National Center for Biotechnology Information; www.ncbi.nlm.nih.gov) for phylogenetic matching.

*Lipid biomarker analysis.* Gas chromatographic profiles of fatty acids (FA), as fatty acid methyl esters (FAME), were used to monitor changes in group-specific biomarker compounds in the surface layers of the greenhouse and field mat communities. A section (~25 $cm^2$ and 1 cm in depth) was removed from a mat in each of the six flow boxes after 4 months, dissected, frozen, and freeze-dried. A similar-sized section was removed from freshly collected mats at the field site in Guerrero Negro in both December 1998 and June 2001. The sections from the field-collected mats were dissected shortly after collection, frozen, and returned to NASA Ames Research Center where they were freeze-dried and processed.

Field and greenhouse mat communities were dissected and processed as follows. The flocculent orange material on the surface of the mat was removed by scraping the surface with a spatula. An exposed leathery layer of the mat, containing extremely high densities of the filamentous cyanobacterium *M. chthonoplastes* (hereafter called the *Microcoleus* layer), ~1–1.5 mm thick, was then separated using a razor blade from the darker-colored gelatinous material that composes the undermat. The freeze-dried mat layers were ground using a glass mortar and pestle. Total lipid extracts were prepared by a Bligh and Dyer single-phase modification (Jahnke *et al.,* 1992). Multiple extractions of the cell material recovered by centrifugation were done until no further pigment coloration was apparent (normally four or five times). A polar fraction (phospholipids and some glycolipids) was prepared by precipitation in cold acetone. The remaining acetone-soluble lipids were separated by thin-layer chromatography using a methylene chloride solvent system (Jahnke *et al.,* 1992). The remaining glycolipids present in the origin zone (0–1 cm) of the thin-layer chromatography plate and the sterols (~2.5–3.5 cm) were recovered from the silica gel by Bligh and Dyer extraction. The polar lipid fractions were pooled, and FAME were prepared by a mild alkaline methanolysis procedure (Jahnke *et al.,* 2001). Gas chromatography–mass spectrometry analyses of FAME or sterols as trimethylsilyl esters were performed using an HP 5890 gas chromatograph equipped with a J&W DB-5ms (30 m × 0.25 mm, 0.25-$\mu$m film) capillary column and an HP 5971 mass-selective detector. Identification of individual compounds was by a combination of standard compounds, published spectra, and relative retention times. FAME were quantified using an Agilent 6890 gas chromatograph equipped with a flame ionization detector and HP-5 (30 m × 0.32 mm, 0.25-$\mu$m film) capillary column. Methyltricosanoate (FAME) was used as an internal standard. Chromatographs were programmed to operate for FAME from 60°C to 120°C at 10°C/min, then at 2°C/min from 120°C to 280°C. Total organic carbon (TOC) and stable isotope composition ($\delta^{13}C$ and $\delta^{15}N$) for biomass was determined using a Carlo Erba CHN EA1108 elemental analyzer interfaced to a Finnigan Delta Plus XL isotope ratio mass spectrometer (Jahnke *et al.,* 2001).

### *Fluxes of oxygen estimated by microsensor measurements*

Net fluxes of oxygen across the mat surface ($J$) were calculated according to Fick's first law of diffusion (Berner, 1980):

$$J = -\phi D_s \, (\partial C/\partial z)$$

where $\partial C/\partial z$ is the change in oxygen concentration with depth near the mat–water interface in ($\mu M/\mu$m), $D_s$ is the sediment (mat in this case) diffusion coefficient ($cm^{-2}$ $s^{-1}$), and $\phi$ is the porosity (volume of water/total volume of water and sediment). $\phi D_s$ within the mat was estimated as follows: For each salinity treatment, a high-resolution (50-$\mu$m step) vertical profile through the diffusive boundary layer (DBL) and the mat was made. $D_0$ (the free solution diffusion coefficient) in the DBL was calculated based on salinity and temperature of the water column at the time of the profile using the equations of Li and Gregory (1974). Since $\phi$ in water is 1 by definition, $\phi D_0$ in the DBL is known. $\phi D_s$ in the mat was then estimated as $(\partial C/\partial z)\, \phi D_0$ (in DBL)/$(\partial C/\partial z)$ (in mat). Mat $\phi D_s$ estimated in this way was similar to published values (Glud *et al.,* 1995; Wieland *et al.,* 2001), $\sim 10^{-5}$.

### *Fluxes of oxygen, dissolved inorganic carbon (DIC), methane, and hydrogen*

Fluxes of oxygen ($O_2$) and DIC between the mats and the overlying water were measured us-

ing glass benthic flux chambers that allowed unimpeded illumination of the surface, with no appreciable (<1°C) heating of the chamber. The chamber design and operation follow those of Canfield and Des Marais (1993). Briefly, each glass chamber (covering an area of mat ~0.019 or 0.012 $m^2$) was fitted with a central stirring paddle and two sampling ports with septa. The glass paddle rotated at a constant rate of 4.5 rpm. Chamber incubations were conducted for full 24-h daily cycles, taking samples by syringe every 6 h. When deployed at sunrise, each chamber was injected with ~100 mL of pure nitrogen ($N_2$) gas to create a headspace to sample at noon and before sunset for acquisition of gas samples ($O_2$, $CH_4$, $H_2$, etc.). At sunset, each chamber was redeployed and injected with 70 mL of $N_2$ and 30 mL of $O_2$ to accommodate $O_2$ demand during the night. Samples were taken at midnight and before sunrise. Dissolved and headspace $O_2$ values were measured using a Clark-style electrode with an internal reference mounted inside a 21-gauge syringe needle (model 768, Diamond General Development Corp.) and a gas chromatograph, respectively. The gas chromatograph (Shimadzu GC-14A) was fitted with a thermal conductivity detector and a CTRI column (Alltech Associates, Deerfield, IL) held at 25°C. Helium, at a flow rate of 30 mL/min, was the carrier gas. DIC samples (5 mL) were filtered and analyzed in triplicate using a "flow injection analyzer" (Hall and Aller, 1992), where a sample was injected into an acidified aqueous solution that subsequently flows past a gas-permeable membrane. Carbon dioxide from the acidified DIC sample traverses this membrane and enters an alkaline solution that subsequently flows through a conductivity detector.

### *Hydrogen partial pressures*

While actively photosynthesizing, mats generate small (~1-$\mu$L) bubbles that are retained at the mat surface with residence times of tens of minutes. These bubbles were collected by means of a 3-mL plastic syringe with a plastic pipette tip lodged in the luer fitting (flaring outward, to form a collecting funnel). When filled with water and submerged, this apparatus allows individual bubbles to be picked from the mat surface, without atmospheric contamination, and pooled to a volume of 10–25 $\mu$L. The pooled bubble gas is immediately subsampled with a gas-tight volumetric syringe and quantified by gas chromatography with HgO-reduction detection (model RGA-3, Trace Analytical, Sparks, MD). The time from sample collection to analysis was generally <30 s. Partial pressures in bubble samples were determined by comparison with standards prepared by serial dilution of pure $H_2$ into $N_2$ (Hoehler *et al.,* 1998). Precision and accuracy are typically about ±5% for sample volumes in the range of 10–25 $\mu$L.

## RESULTS

### *The greenhouse facility as a simulation of the natural environment*

Microbial mats kept in the greenhouse facility retained an overall appearance remarkably similar to that of freshly collected mats. In particular, no evidence of the mat "greening," in which motile cyanobacteria migrate to the surface of the mat (Bebout and Garcia-Pichel, 1995), was apparent. During the first few weeks of greenhouse incubation, there was a notable increase in the abundance of loosely attached microbial "floc" at the surface of the mats, as well as the development of small dark green spots containing large numbers of cyanobacterial filaments in some mats. However, after the first 2 months, the loose floc disappeared, and the mat surface was smooth and homogeneous in appearance once again. Extensive, but nonquantitative, microscopic observations revealed no major changes in community composition. More specifically, the major populations of cyanobacteria did not seem to change, and *M. chthonoplastes* remained the dominant phototroph in all of the sections of mat characterized microscopically.

Molecular analyses based on 16S rRNA genes through DGGE fingerprinting were consistent with the absence of significant shifts in the community. The banding pattern of DNA extracted from the greenhouse mats was essentially identical to that of freshly collected mats (Fig. 2). Two major bands were present in all of the mat samples (Band *b* and Band *c*). In the greenhouse treatments (Fig. 2A), Band *c* represented 84% of the observed cyanobacterial diversity, gauged as a percentage of total PCR amplificate, while Band *b* represented 10%. These results are consistent with the structure of field samples (Fig. 2B), where Band *c* represented 79% of the observed diversity with

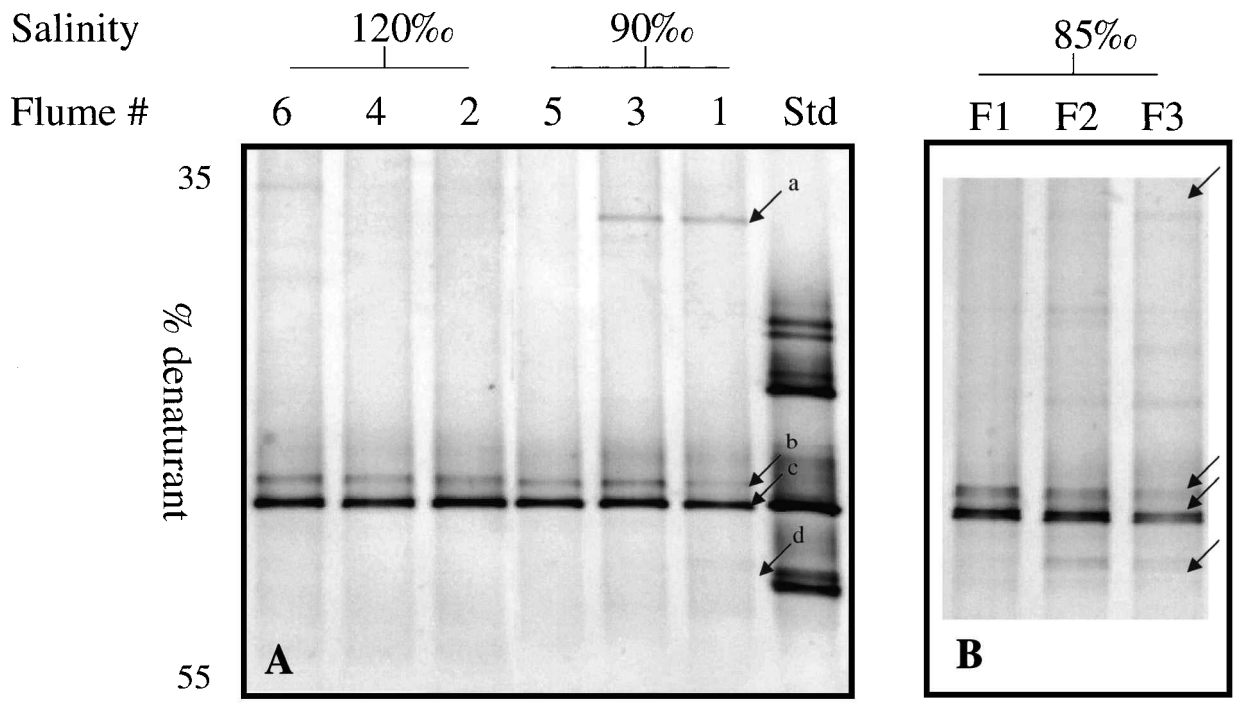


**FIG. 2. DGGE fingerprints of PCR-amplified cyanobacterial 16S rRNA genes of the six flume treatments (A) and field samples (B).** Arrows indicate bands used for further analysis of the fingerprints. Bands *b*, *c*, and *d* were excised, re-amplified, and sequenced.

Band *b* accounting for 18%. Two other minor bands were found, but not in all treatments. Band *a* was present in three of the six greenhouse samples and in the field samples, accounting for 3% and 2% of the observed diversity, respectively. Band *d* was found in all six greenhouse samples at much lower levels (0.8%), and accounted for 1.2% of the observed diversity in the field samples. BLAST similarity searches for the sequenced bands (~380 bp in length) were performed. Band *b* had no close matches to any cultured cyanobacterium (only 89% similar to *Oscillatoria amphigranulata* strain 23-2, a typical distance between bacterial genera), but did match an unidentified, uncultured cyanobacterium from a microbial mat in Solar Lake, Sinai Peninsula, Egypt (Abed and Garcia-Pichel, 2001) with 94% similarity. The BLAST results for the remaining two bands yielded very high similarity (99%) to known cultured cyanobacteria. Band *c* matched the *M. chthonoplastes* cluster (Garcia-Pichel *et al.*, 1996) and Band *d* matched *Euhalothece* sp. strain MPI 95AH13 (Garcia-Pichel *et al.*, 1998). Though we were unable to sequence it, Band *a* most likely represents a diatom plastid (according to previous research and band placement in the denaturant gradient).

The compositions of the total esterified FA (TEFA) in natural and greenhouse mats were in most respects similar for both the surface and underlying *Microcoleus* layer (Table 1). The amounts of TEFA recovered for the individual mat samples were reasonably consistent. The majority of this TEFA consisted of *n*-16:0, *n*-16:1, and *n*-18:1, which together accounted for 60–77% of all FA. Smaller amounts of other straight-chain saturated and unsaturated FA (i.e., *n*-14:0, *n*-17:0, *n*-18:0, *n*-17:1, *n*-20:1, *n*-20:2) together with various terminally branched FA (*i*-14:0, *i*-15:0, *ai*-15:0, *i*-16:0, *i*-17:1, *i*-17:0, *ai*-17:0) were present in relatively uniform amounts in all samples. However, subtle differences for TEFA compositions in the surface layer and underlying *Microcoleus* layer of natural mats, which were also apparent in the greenhouse mats even after 4 months of experimental treatment (Fig. 3), were noted. The surface layer tended to have higher levels of *iso*-15:1 and *iso*-16:1 than the *Microcoleus* layer. In natural mat, these two *iso*-FA were composed primarily (90%) of Δ4 positional isomers, previously identified in field-collected *Nostoc* spp. (Potts *et al.*, 1987). All surface layers (in both natural and greenhouse mats) also contained small amounts

Table 1. Composition of Two Natural Mats from the Area 4 Mat Dissected at Guerrero Negro and of Mats Collected from the Same Area After Maintenance in the Flume System for ≥4 Months

| | *12/98 P4n5*[1] | | *90‰ flume* | | *120‰ flume* | | *6/01 P4n5*[1] | |
|---|---|---|---|---|---|---|---|---|
| | *Surface* | Microcoleus | *Surface* | Microcoleus | *Surface* | Microcoleus | *Surface* | Microcoleus |
| Ester-linked FA (mg $g^{-1}$ TOC) | 17.76 | 31.80 | 25.67 | 23.38 | 26.52 | 27.85 | 30.87 | 22.09 |
| C/N Ratio | 9.8 | ND | 9.4 | 9.2 | 12.1 | 9.6 | ND | ND |
| $\delta^{13}C$ (‰) | −10.72 ± 0.04 | −10.23 ± 0.28 | −9.01 ± 0.05 | −10.59 ± 0.13 | −9.70 ± 0.17 | −10.50 ± 0.1 | −8.02 ± 0.07 | −10.5 ± 0.65 |
| $\delta^{15}N$ (‰) | −0.13 ± 0.4 | ND | −1.27 ± 0.06 | −0.92 ± 0.38 | −0.23 ± 0.35 | −0.26 ± 0.18 | ND | ND |

Error estimates shown indicate instrumental precision. Samples labeled ND were too small to permit a reliable analysis.
[1]Collected in December 1998 and June 2001 from the field site, Pond 4 near Area 5.

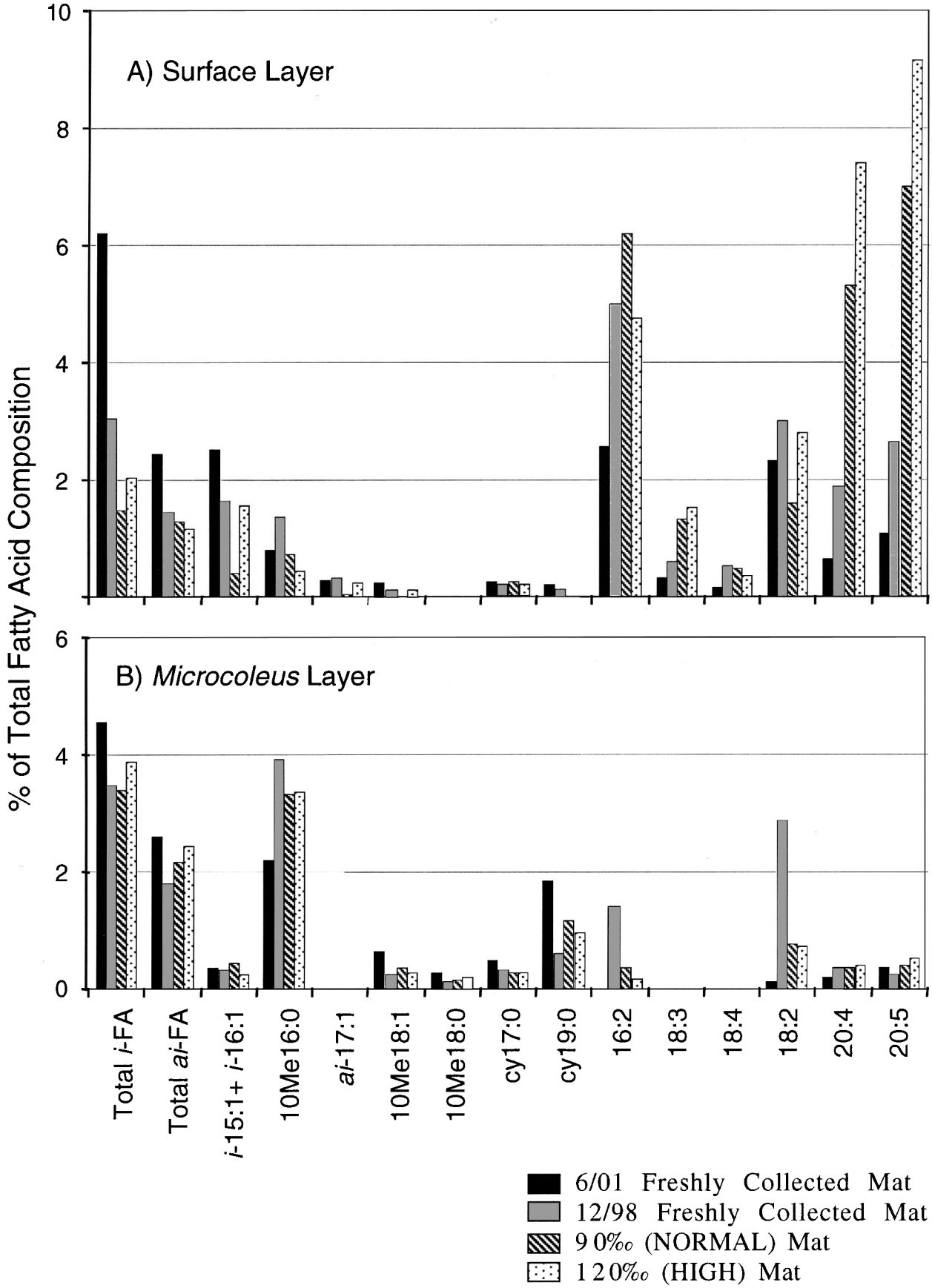


**FIG. 3. Relative distribution of various FA characteristic of the surface layer (A) and/or the underlying *Microcoleus* layer (B) for two natural mats collected from Pond 4 near Area 5 in June 2001 (black bars) and December 1998 (gray bars), and for similar mats maintained for ≥4 months in flumes at salinities of 90‰ (hatched bars) or of 120‰ (dotted bars).**

of *anteiso*-17:1, which was not detected in the *Microcoleus* layer. The most striking difference in the surface layer, however, was the presence of relatively large amounts of several polyunsaturated FA (PFA) (*n*-16:2, *n*-18:2, *n*-18:3, *n*-18:4, *n*-20:4, and *n*-20:5). The more highly unsaturated $C_{20}$ FA are generally considered diatom biomarkers (Cobelas and Lechado, 1989). The lower *Microcoleus* layer was also considerably enriched in several FA. Most pronounced were a 10-methyl-16:0 associated with some sulfate-reducing bacteria (Dowling *et al.,* 1986; Kohring *et al.,* 1994) and a *cy*-19:0 that has been used as a biomarker for *Thiobacillus* spp. (Kerger *et al.,* 1986). In addition, microbial mats maintained in the greenhouse retained the carbon and nitrogen stable isotopic composition of recently collected mats (Table 1).

Measurements of rates of biogeochemical cycling in greenhouse mats were similar to rates measured on freshly collected mats (Table 2). Profiles of oxygen concentration within the greenhouse mats resembled those obtained *in situ,* in both absolute concentration and distribution with depth (data not shown). Oxygen fluxes to the water column, calculated from the concentration gradients of these profiles, agreed with oxygen fluxes calculated from *in situ* profiles over a wide range of light intensities (Fig. 4). Similarly, net rates of $O_2$ and DIC production and consumption as determined using flux measurements were similar to those measured in freshly collected mats (Table 2) after allowances were made for the relationship between rates of photosynthesis and seasonally-dependent levels of illumination in the greenhouse. Fluxes of methane from the greenhouse mats were reduced to 60% of the value measured in freshly collected mats and were essentially equal day and night (Table 2). In gas bubbles collected at the mat surface, $H_2$ partial pressures in the low-salinity control mats were very similar to those observed in the field (Table 2).

### *The greenhouse as a facility for experimental manipulations*

Over the course of the experiment, dramatic differences in the appearance of mats maintained at *in situ* (NORMAL = 90‰) and elevated (HIGH = 120‰) salinities became apparent. Mats held at high salinities assumed a much more orange color than those incubated at lower salinities. A change in color can result from physiological (photopigment) changes in an unchanged community or population shifts. It is known that increased salinity promotes increasingly oxidative conditions (Garcia-Pichel *et al.,* 1999) and that *M. chthonoplastes* can respond to increased salinity by increasing the cellular levels of carotenoid (López-Cortés, 1990). It is important to note, however, that in natural field mats yellow-orange mats are typically associated with the dominance of cyanobacteria from the *Halothece* cluster.

Nonquantitative microscopic observations revealed an increase in the abundance of unicellular cyanobacteria that resembled the *Halothece* type at the surface of the HIGH salinity mats relative to those maintained at NORMAL salinity. Initial DGGE analyses supported this observation, with a faint novel band attributable to *Halothece,* which appeared in samples collected from all three HIGH salinity greenhouse mat samples (data not shown). However, these initial DGGE samples had been compromised by an accidental thawing. The second set of samples, taken at the same time but not thawed before DNA extraction, did not show this band (Fig. 2). Rather, this second set of samples showed similar fingerprints for all greenhouse samples, regardless of the treatment. Upon further investigation, we found that thawing and refreezing of mat samples before DNA extraction caused the preferential breakage of large-celled *M. chthonoplastes,* and the subsequent degradation of its DNA. Because *M. chthonoplastes* provides the majority of template for PCR amplification, DGGE analyses of samples that had been thawed yielded a high-resolution fingerprint of the community members present at low numbers. It was only in such analyses that we could detect community shifts in the form of new bands appearing in all HIGH salinity greenhouses (data not shown). Sequencing and phylogentic analyses of these novel bands revealed that the new community members belonged to the *Halothece* cluster of extremely halotolerant, unicellular cyanobacteria (Garcia-Pichel *et al.,* 1998). Thus we may have been witnessing an incipient community shift, but not a full replacement of the principal cyanobacterial populations.

Some differences between the NORMAL and HIGH salinity mats, and between greenhouse and freshly collected mats, were apparent in the FA composition. An increase in the diatom population in the HIGH salinity mats was readily documented by increased amounts of two diatom

TABLE 2. MEASUREMENTS OF BIOGEOCHEMICAL PROCESSES IN FRESHLY COLLECTED MATS AND MATS MAINTAINED IN THE GREENHOUSE FACILITY AT NORMAL AND HIGH SALINITIES

| | | *Greenhouse-maintained mats* | | | | | |
|---|---|---|---|---|---|---|---|
| | | *June 14–15, 2000* | | *July 6–7, 2000* | | *November 8–9, 2000* | |
| | *Freshly collected mat May 19–20, 2000* | *NORMAL* | *HIGH* | *NORMAL* | *HIGH* | *NORMAL* | *HIGH* |
| Temperature (°C) | | | | | | | |
| Nighttime | 16 | 19 | 19 | 16 | 16 | 16 | 16 |
| Daytime | 16 | 21 | 21 | 19 | 19 | 19 | 19 |
| DIC flux (mmol $m^{-2}h^{-1}$) | | | | | | | |
| Nighttime | 2.60 (0.02) | 4.86 (0.36) | — | 3.6 (N/A) | 3.07 (0.05) | 3.8 (N/A) | 3.3 (N/A) |
| Daytime | −3.29 (0.14) | −6.86 (0.15) | — | −5.6 (N/A) | −3.74 (0.08) | −2.1 (N/A) | −0.6 (N/A) |
| Oxygen flux (mmol $m^{-2}h^{-1}$) | | | | | | | |
| Nighttime | −3.52 (0.01) | −4.45 (0.02) | — | −2.4 (N/A) | −2.41 (0.01) | −4.00 (0.25) | −3.34 (0.01) |
| Daytime | 3.49 (0.62) | 7.20 (0.31) | — | 5.6 (N/A) | 3.98 (0.04) | 4.66 (0.37) | 4.43 (0.02) |
| Methane flux (nmol $m^{-2}h^{-1}$) | | | | | | | |
| Nighttime | 381 (5.47) | 179 (23.6) | — | 180 (43.3) | 170 (25.8) | 152 (3.14) | 524 (32.1) |
| Daytime | 328 (27.6) | 214 (63.5) | — | 176 (68.3) | 174 (11.6) | 200 (7.38) | 653 (21.1) |
| [$H_2$] (ppm) | | | | | | | |
| Steady-state | 10.7 (3.3) | 0.54 (0.16) | — | 0.67 (0.18) | 0.28 (0.08) | — | — |
| Bubble | 4.6 (2.9) | 4.3 (2.0) | 2.9 (1.0) | 4.0 (0.0076) | 1.1 (0.12) | — | — |
| | $n = 26$ | $n = 8$ | $n = 6$ | $n = 2$ | $n = 2$ | | |

Values in parentheses represent the SD of mean values. For flux measurements, $n = 2$. The number of replicates for hydrogen bubble measurements is indicated. An SD value of N/A indicates a flux measurement of a single sample ($n = 1$). Temperatures at which the measurements were made are also indicated.

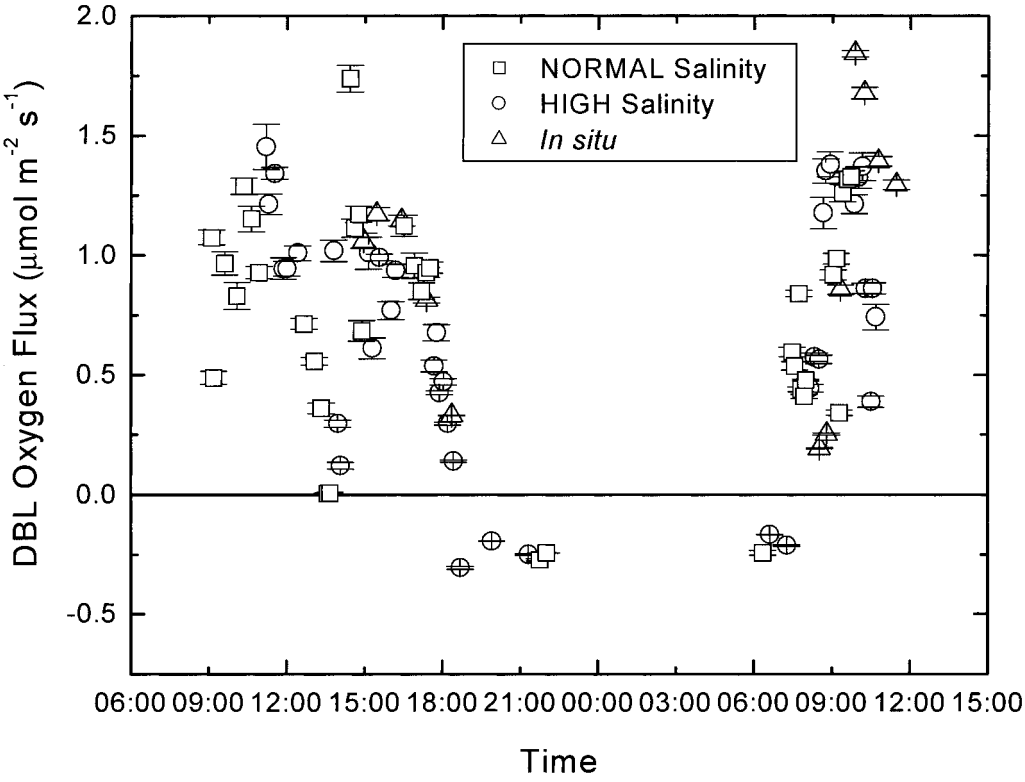


**FIG. 4. Microelectrodes were used to monitor oxygen fluxes across the Area 4 mat surface–water interface during greenhouse [NORMAL (squares) and HIGH (circles) salinity] and *in situ* (triangles) experiments.** Positive fluxes indicate net flux of photosynthetically-generated oxygen out of the mat, while negative fluxes indicate net oxygen consumption. Error bars are SE values. Mats maintained in the greenhouse retain the general diel pattern observed *in situ*, including a morning peak in photosynthesis. Note shading events caused by greenhouse window crossbars resulting in temporary light limitation of photosynthesis in small areas of the greenhouse mats (e.g., at 13:30 on Day 1 and at 10:30 on Day 2).

biomarkers: the PFA 20:4 and 20:5, and the sterol composition. Together 20:4 and 20:5 accounted for 4.38 mg $g^{-1}$ TOC in the HIGH salinity mats and only 3.16 mg $g^{-1}$ TOC in the NORMAL salinity mats. Both of these values are considerably higher than the natural mat samples (~0.6 mg $g^{-1}$). Sterols, a direct indication of the presence of microeukaryotes in these mat samples, were also more abundant in the HIGH salinity treatment with 1.20 mg $g^{-1}$ versus 0.74 mg $g^{-1}$ for NORMAL salinity mats. The two sterols that serve as diatom biomarkers, 24-methylcholesta-5-en-3$\beta$-ol and 24-methylcholesta-5,22-dien-3$\beta$-ol (Volkman, 1986), accounted for ~80% of the total in both greenhouse samples.

There were no differences observed in oxygen profiles in the NORMAL and HIGH salinity mats (Fig. 5). Fluxes of $O_2$ were measured at the outset (June 2000) of the parallel treatment of the mats at two salinities, and 5 months later (November 2000). In both cases, no differences in $O_2$ fluxes were apparent between the two salinity treatments with regard to the rate of export of $O_2$ to the overlying water column during the day, or the uptake of $O_2$ at night (Table 2). In contrast, rates of methane production from the NORMAL and HIGH salinity mats, which showed no difference for the majority of time the experiment was running, differed at the last sampling (November 8–9, 2000), with higher rates recorded in the normal-salinity treatment. $H_2$ partial pressure in photosynthetic surface bubbles from the HIGH salinity mats was about half that in the NORMAL salinity mats after running the experiment for 5 months.

## DISCUSSION

For a period of at least 1 year, microbial mats maintained in the greenhouse facility resembled field-collected microbial mats with respect to

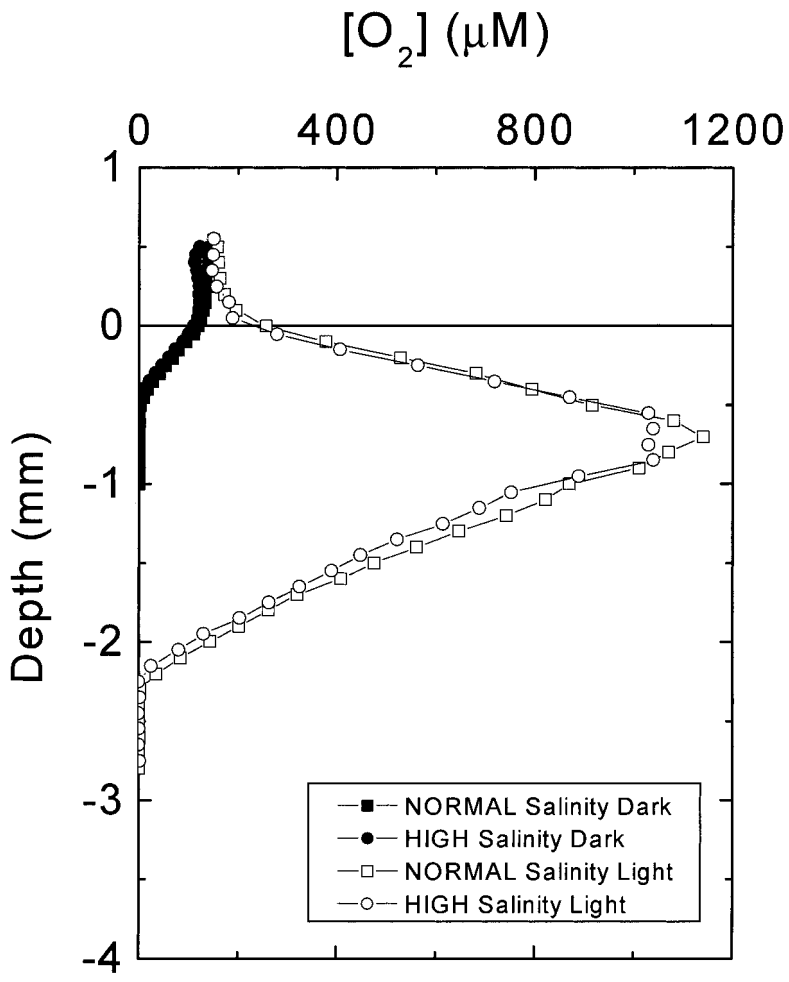


**FIG. 5. Oxygen microelectrode profiles within microbial mat in the daytime (1000h, open symbols) and nighttime (2200h, solid symbols).** Little difference can be seen in profiles taken in mats incubated at NORMAL (squares) and HIGH (circles) salinity.

their overall appearance, cyanobacterial community composition, and rates of biogeochemical cycling. High rates of activity of microbial populations in mats contributed to the adaptability of these ecosystems. However, this attribute also makes the preservation of mat systems in their original, natural states especially challenging. The phenomenon known as "greening," in which motile cyanobacteria migrate to the surface of the mats and remain there in response to lowered irradiance, is common in mats maintained under artificial illumination (Bebout and Garcia-Pichel, 1995). For example, when removed from their natural environment and maintained in large outdoor ponds, microbial mats collected from hypersaline Solar Lake, Sinai, Egypt became "overgrown" with populations of cyanobacteria that are not necessarily well-represented *in situ* (Abed and Garcia-Pichel, 2001).

Oxygen microprofiles, measured using microelectrodes, and oxygen and carbon fluxes, measured using flux chambers, were found to be comparable in greenhouse and freshly collected natural mats. While it is reassuring to observe this similarity in mat net community metabolism, it is likely that these parameters are among the least sensitive to change since measurements of net carbon and oxygen flux integrate the rates of metabolic activity of most of the microorganisms in the community. Increases in the activity of one group of microorganisms may be compensated for by decreases in the activity of others. We also measured a close similarity between greenhouse and *in situ* bubble $H_2$ partial pressures. $H_2$ partial pressures in bubbles are extremely sensitive to changes in the environment of photosynthesis in the uppermost mat layer. For example, mats removed from their native pond and placed under conditions of high solar irradiance and low or no water flow frequently exhibited an increase in bubble $H_2$ partial pressures of up to 2 orders of magnitude. The combination of light and flow

regimens appears to exert strong and instantaneous control on bubble $H_2$ partial pressures by setting the balance between diffusive DIC supply and light intensity (Lambert and Smith, 1980; Houchins, 1984). The fact that little or no difference in bubble $H_2$ partial pressures was apparent between greenhouse and natural mats suggests that the basic flow and light regimens of the natural environment are recreated to a very high degree in the greenhouse setting.

We believe that the greenhouse approach documented here is among the most successful of the efforts to date to produce an environment appropriate for the long-term study of these important microbial communities. When compared with previous efforts to maintain microbial mats, our results indicate that two factors—water flow and the light regime—are likely to be more important than others in simulating the field environment. We discuss in more detail the importance of these two factors in our greenhouse facility.

The importance of flow in microbial mat metabolism has been recognized for at least a decade (Jørgensen, 1994; Boudreau and Jørgensen, 2001). The DBL, a thin (~0.5 mm) layer of stagnant water, is situated at the interface between any microbial mat community and the water column, even under conditions of high water flow. The transport of all solutes between the water column and the mat occurs exclusively by molecular diffusion through the DBL. Therefore the thickness of this layer sets the rates at which this exchange may take place. Rates of activity, including rates of primary production in microbial mat communities, may be controlled by the rate at which carbon dioxide and oxygen diffuse across the DBL (Garcia-Pichel *et al.,* 1999).

In the greenhouse facility, water was constantly circulated over the mats. The flow velocity was set to ~5 cm $s^{-1}$ by adjusting the output of our water pumps with valves, and measured and maintained by periodic observations of the transit of small particles or bubbles (through a measured distance in the flow box over a given period of time). We chose a value of 5 cm $s^{-1}$ for the greenhouse experiments as (1) it was a reasonable approximation of average *in situ* values and (2) that flow velocity is used in a large number of published microelectrode measurements in microbial mats (Revsbech and Jørgensen, 1986), which facilitated the ability to compare our results with those of others.

Previous work with these mats revealed that, compared with the dramatic change in DBL thickness that occurs as flow velocities increase from 0 (stagnant) to 1–3 cm $s^{-1}$, the DBL thickness is relatively constant once flow velocities exceed 1–3 cm $s^{-1}$ (Jørgensen and Des Marais, 1990). Therefore, flow variations around the 5 cm $s^{-1}$ value will minimally affect the fluxes in and out of the mat. For the flux chamber measurements reported here, motor speeds were adjusted to drive the paddles to produce similar (5 cm $s^{-1}$) flow velocities, which were also estimated by timing the transit of small particles within the flux chambers across the surface of the mats. Actual *in situ* flow velocities, also measured by observations of naturally occurring particles underwater by divers, range from 0 (in the morning before the wind comes up) to >20 cm $s^{-1}$ under windy afternoon conditions, though these values should be regarded as rough estimates owing to the turbulent nature of the flow and the difficulty inherent in making the observations. No attempt was made in the greenhouse to simulate these daily fluctuations in flow velocities. However, the similarity of microelectrode-based measurements of DBL thickness (not shown) and microelectrode profile-based oxygen fluxes to those measured *in situ* (Fig. 4) suggests that the greenhouse flume system closely reproduces the environmental flow field and DBL control on mat–water solute exchange.

In photosynthetic microbial mats, all of the energy necessary for growth and maintenance of the community is ultimately derived from the sun. Oxygen production and consumption by these phototrophic organisms, as well as their sensitivity to UV radiation, determine the physical structure of the entire mat community. Furthermore, many mat microorganisms are motile, utilizing light and/or UV radiation as a cue to adjust their position in the mats vertically (Castenholz, 1994; Bebout and Garcia-Pichel, 1995). Therefore, these mats are highly sensitive to changes in PAR (light within the wavelength range from 400 to 700 nm). The use of artificial illumination to drive photosynthetic activity in microbial mats over longer periods of time is not attractive from a logistical perspective owing to the large amounts of heat that is generated. In addition, sources of artificial light rarely reproduce the high irradiance, and (even more rarely) the spectral composition of natural sunlight. For both of these reasons, the use of natural sunlight is preferred for the mainte-

nance of these microbial communities. Use of a greenhouse facility for microbial mat maintenance is also the most cost-effective way to deliver the required visible and UV radiation to microbial mat communities, particularly when large areas of mat are required for destructive sampling and/or large numbers of replicate measurements.

Mats maintained in the greenhouse facility have access to natural solar radiation filtered only through OP-4 acrylic and a few centimeters of water. Therefore, both the total PAR irradiance and the exact spectral composition of that PAR are essentially unchanged from that of sunlight. The difference in latitude between our greenhouse and the field site, as well as the absence of a 1-m water column in the greenhouse, contributed to making the irradiance at the surface of the greenhouse mats similar to that *in situ*. For example, the irradiance measured at the field site (on cloud-free days at high noon) = 1,845 ± 196.9 $\mu$E $m^{-2}$ $s^{-1}$ (average reading from four field trips, in May 2000, June 2001, October 2001, and September 2002). Attenuation of light by the water column resulted in values measured at the mat surface (on those same cloud-free days) of 1,130 ± 301.9 $\mu$E $m^{-2}$ $s^{-1}$. In comparison, the average reading at the mat surface in the greenhouse was 1,005 ± 396.2 $\mu$E $m^{-2}$ $s^{-1}$ (mean ± SD, $n = 548$, values recorded at 10-min intervals from 1200h to 1300h from June 2001 through September 2001). The greenhouse irradiance record includes cloudy days, but these were relatively few in number owing to the relatively clear summer skies at NASA Ames Research Center.

Microbial mats *in situ* are likely to experience some changes in the spectral composition of light incident upon their surface (relative to sunlight) due to particulates present in the water column. These changes in spectral composition of the incoming PAR (relative to sunlight) vary (e.g., with time of year due to changes in the community composition of phytoplankton in the salterns, and with time of day due to wind-driven resuspension of detrital material). No attempt was made to simulate these changes in spectral composition in the greenhouse. Owing to the high diversity of phototrophic organisms in mats, and the wide variety of pigments used by those organisms to capture light for photosynthesis, the total quantity of photons incident upon a mat community is of far greater importance for community metabolism than the exact spectral composition of the incoming radiation (Prufert-Bebout *et al.*, 1998). Additionally, cyanobacterial motility and photosynthetic state transitions provide for efficient use of the rapidly changing spectral compositions within microbial mat communities over the 1,000-$\mu$m depth range, within which visible irradiance is extinguished (Ploug *et al.*, 1998; Prufert-Bebout *et al.*, 1998).

Future modifications in greenhouse flow and light regimens may further improve our ability to simulate the field environment. The one potentially significant difference in community composition observed between greenhouse and natural mats, namely, the apparent increase in the abundance of diatoms in surface layers as suggested by the FAME biomarker data, may, in fact, be explained by differences in the flow regimen experienced by mats incubated in the greenhouse relative to *in situ* conditions. In the greenhouse, the flow of water over the mats, while reproducing natural flow velocities and DBL thickness, occurs 24 h a day. In the field environment, water flow over mats is primarily wind-driven and, as such, is variable over the course of the day. Strong winds are characteristic of the afternoon, as rising warm air is replaced by strong onshore breezes. At night, and into the morning, there is very little wind and, therefore, a much lower flow of water over the mats. Recently, we have documented a density stratification of the ponds at night. This density stratification, in combination with high rates of oxygen consumption by the mat, resulted in a layer of anoxic bottom water several centimeters thick, which persisted until late morning (S.R. Miller, unpublished data). Hydrogen sulfide, produced in the mat by sulfate reduction, reached levels in excess of 185 $\mu M$ in this layer (B. Thamdrup, personal communication). Additionally, we recently documented that temperatures at the mat surface are often several degrees higher than those in the middle of the water column and those that we have been simulating in the greenhouse. This is presumably because of greater heat retention by the sediments underlying the microbial mats in their natural environment. Constant flow over the greenhouse mats would tend to diffuse heat from the surface layers of the mat, resulting in temperatures lower than those recorded *in situ*.

The lack of exposure to anoxic, sulfidic water at night, as well as greenhouse water temperatures lower than those experienced by the mats *in situ*, would tend to increase the abundance of diatoms relative to unicellular cyanobacteria in

the surface layers of the greenhouse mats. The photosynthetic performance of the diatoms may be inhibited *in situ* as a result of the sulfide sensitivity of oxygenic photosynthesis (Oren *et al.,* 1979), and unicellular cyanobacteria from microbial mats are known to grow optimally at relatively high temperatures (Dor and Paz, 1989; Garcia-Pichel *et al.,* 1998). Future work in the greenhouse will investigate the extent to which periodic and/or nighttime periods of low flow, as well as periodic higher temperature excursions, might reduce the tendency of the diatoms to dominate surface layers of the mat.

The microbial mats in our greenhouse simulation facility represent a resource from which we would like to obtain diverse observations and as much data as necessary to address key questions in ecology. To increase the accessibility of the greenhouse to members of our research group, the facility is being transformed into a "collaboratory." The collaboratory will enable a geographically dispersed group of scientists to plan experiments, operate scientific equipment, take experimental measurements, share results, and collaborate in real time with remote colleagues. Within the collaboratory, intelligent software agents will assist in the experimentation process controlling the hardware, troubleshooting, re-cording results, and reporting back to collaborating experimenters. The *xyz* positioning table over the mats is capable of automatically positioning sophisticated instruments at any location over and within the mats. The instrument package currently includes microelectrodes, a light sensor, chlorophyll fluorometer, a surface detection device, and a fiber optic spectrometer. The positioning system and instrumentation package are viewable over the Internet (http://greencam.arc.nasa.gov) via a webcam connected to a computer located in the greenhouse. The advanced automation capabilities in the greenhouse will enable longer-term experimentation, 24 h a day, without the costs associated with extensive human supervision. The remote collaboration capabilities will extend this experimental resource to colleagues not physically present in the greenhouse.

In summary, in addition to reproducing rates of *in situ* biogeochemical processes, greenhouse microbial mats were responsive to manipulations of environmental conditions. Increasing the salinity of water in the greenhouse facility reproduced some of the community composition changes observed in natural mats growing at higher salinities. The differences observed in the salinity responses of natural and greenhouse mats may be consistent with expected differences between field and greenhouse environmental conditions (e.g., differences in temperature and nighttime oxygen and hydrogen sulfide concentrations). Therefore, we are optimistic that this facility may be used not only to maintain mats with natural levels of activity and species composition, but also to explore environmental conditions that are not presently found in the natural environment (e.g., low sulfate and low oxygen environments).

## ACKNOWLEDGMENTS

This study was supported by grants from the NASA Astrobiology Institute, the NASA Exobiology Program, and the NASA Ames Director's Discretionary Fund. The greenhouse *xyz* table was designed and constructed by Dan Andrews and Brian Koss, Code FE, NASA Ames Research Center, and funded by the NASA Intelligent Systems Program. Comments by two anonymous reviewers greatly improved the manuscript.

## ABBREVIATIONS

DBL, diffusive boundary layer; DGGE, denaturing gradient gel electrophoresis; DIC, dissolved inorganic carbon; FA, fatty acids; FAME, fatty acid methyl esters; PAR, photosynthetically available radiation; PCR, polymerase chain reaction; PFA, polyunsaturated fatty acids; TEFA, total esterified fatty acids; TOC, total organic carbon.

## REFERENCES

Abed, A.M.M. and Garcia-Pichel, F. (2001) Long-term compositional changes after transplant in a microbial mat cyanobacterial community revealed using a polyphasic approach. *Environ. Microbiol.* 3, 53–62.

Amann, R.I., Ludwig, W., and Schleifer, K.H. (1995) Phylogenetic identification and *in situ* detection of individual microbial cells without cultivation. *Microbiol. Rev.* 59, 143–169.

Bebout, B.M. and Garcia-Pichel, F. (1995) UVB-induced vertical migrations of cyanobacteria in a microbial mat. *Appl. Environ. Microbiol.* 61, 4215–4222.

Berner, R.A. (1980) *Early Diagenesis: A Theoretical Approach,* Princeton University Press, Princeton, NJ.

Beukes, N.J. and Lowe, D.R. (1989) Environmental control on diverse stromatolite morphologies in the 3000

Myr Pongola Supergroup, South Africa. *Sedimentology* 36, 383–397.

Boon, J.J. (1984) Tracing the origin of chemical fossils in microbial mats: biogeochemical investigations of solar lake cyanobacterial mats using analytical pyrolysis methods. In *Microbial Mats: Stromatolites,* edited by Y. Cohen, R.W. Castenholz, and H.O. Halvorson, Alan R. Liss, New York, pp. 313–342.

Boudreau, B.P. and Jørgensen, B.B., eds. (2001) *The Benthic Boundary Layer: Transport Processes and Biogeochemistry,* Oxford University Press, New York.

Canfield, D.E. and Des Marais, D.J. (1991) Aerobic sulfate reduction in microbial mats. *Science* 251, 1471–1473.

Canfield, D.E. and Des Marais, D.J. (1993) Biogeochemical cycles of carbon, sulfur and free oxygen in a microbial mat. *Geochim. Cosmochim. Acta* 57, 3971–3984.

Canfield, D.E. and Teske, A. (1996) Late Proterozoic rise in atmospheric oxygen from phylogenetic and stable isotope studies. *Nature* 382, 127–132.

Castenholz, R.W. (1994) Microbial mat research: the recent past and new perspectives. In *Microbial Mats: Structure, Development and Environmental Significance,* edited by L.J. Stal and P. Caumette, Springer-Verlag, New York, pp. 265–271.

Cobelas, M.A. and Lechado, J.Z. (1989) Lipids in microalgae. A review. I. Biochemistry. *Grasas Aceites* 40, 118–145.

Des Marais, D.J. (1995) The biogeochemistry of hypersaline microbial mats. *Adv. Microb. Ecol.* 14, 251–274.

Des Marais, D.J. and Canfield, D.E. (1994) The carbon isotope biogeochemistry of microbial mats. In *Microbial Mats: Structure, Development and Environmental Significance,* edited by L.J. Stal and P. Caumette, Springer-Verlag, New York, pp. 289–298.

Des Marais, D.J., Harwit, M.O., Jucks, K.W., Kasting, J.F., Lin, D.N.C., Lunine, J.I., Schneider, J., Seager, S., Traub, W.A., and Woolf, N.J. (2002) Remote sensing of planetary properties and biosignatures on extrasolar terrestrial planets. *Astrobiology* 2, 153–181.

Dor, I. and Paz, N. (1989) Temporal and spatial distribution of mat microalgae in the experimental solar ponds, Dead Sea area, Israel. In *Microbial Mats: The Physiological Ecology of Benthic Microbial Communities,* edited by Y. Cohen and E. Rosenberg, American Society for Microbiology, Washington, DC, pp. 114–122.

Dowling, N.J.E., Widdel, F., and White, D.C. (1986) Phospholipid ester-linked fatty acid biomarkers of acetate-oxidizing sulphate-reducers and other sulphide-forming bacteria. *J. Gen. Microbiol.* 132, 1815–1825.

Garcia-Pichel, F., Prufert-Bebout, L., and Muyzer, G. (1996) Phenotypic and phylogenetic analyses show *Microcoleus chthonoplastes* to be a cosmopolitan cyanobacterium. *Appl. Environ. Microbiol.* 62, 3284–3291.

Garcia-Pichel, F., Nübel, U., and Muyzer, G. (1998) The phylogeny of unicellular, extremely halotolerant cyanobacteria. *Arch. Microbiol.* 169, 469–482.

Garcia-Pichel, F., Kühl, M., Nübel, U., and Muyzer, G. (1999) Salinity-dependent limitation of photosynthesis and oxygen exchange in microbial mats. *J. Phycol.* 35, 227–238.

Garret, P. (1970) Phanerozoic stromatolites: noncompetitive ecological restriction by grazing and burrowing animals. *Science* 169, 171–173.

Glud, R.N., Jensen, K., and Revsbech, N.P. (1995) Diffusivity in surficial sediments and benthic mats determined by use of a combined $N_2O$-$O_2$ microsensor. *Geochim. Cosmochim. Acta* 59, 231–237.

Hall, P.O.J. and Aller, R.C. (1992) Rapid, small-volume, flow injection analysis for $\Sigma CO_2$ and $NH_4^+$ in marine and freshwaters. *Limnol. Oceanogr.* 37, 1113–1119.

Hoehler, T.M., Alperin, M.J., Albert, D.B., and Martens, C.S. (1998) Thermodynamic control on $H_2$ concentrations in an anoxic marine sediment. *Geochim. Cosmochim. Acta* 62, 1745–1756.

Hoehler, T.M., Bebout, B.M., and Des Marais, D.J. (2001) The role of microbial mats in the production of reduced gases on the early Earth. *Nature* 412, 324–327.

Holland, H.D. (1984) *The Chemical Evolution of the Atmosphere and Oceans,* Princeton University Press, Princeton, NJ.

Houchins, J.P. (1984) The physiology and biochemistry of hydrogen metabolism in cyanobacteria. *Biochim. Biophys. Acta* 768, 227–255.

Jahnke, L.L., Stan-Lotter, H., Kato, K., and Hochstein, L.I. (1992) Presence of methyl sterol and bacteriohopanepolyol in an outer-membrane preparation from *Methylococcus capsulatus* (Bath). *J. Gen. Microbiol.* 138, 1759–1766.

Jahnke, L.L., Eder, W., Huber, R., Hope, J.M., Hinrichs, K.-U., Hayes, J.M., Des Marais, D.J., Cady, S.L., and Summons, R.E. (2001) Signature lipids and stable carbon isotope analyses of Octopus Spring hyperthermophilic communities compared with those of *Aquificales* representatives. *Appl. Environ. Microbiol.* 67, 5179–5189.

Jørgensen, B.B. (1994) Diffusion processes and boundary layers in microbial mats. In *Microbial Mats: Structure, Development and Environmental Significance,* edited by L.J. Stal and P. Caumette, Springer-Verlag, New York, pp. 243–253.

Jørgensen, B.B. and Des Marais, D.J. (1990) The diffusive boundary layer of sediments: oxygen microgradients over a microbial mat. *Limnol. Oceanogr.* 35, 1343–1355.

Jørgensen, B.B., Revsbech, N.P., Blackburn, T.H., and Cohen, Y. (1979) Diurnal cycle of oxygen and sulfide microgradients and microbial photosynthesis in a cyanobacterial mat sediment. *Appl. Environ. Microbiol.* 38, 46–58.

Kerger, B.D., Nichols, P.D., Antworth, C.P., Sand, W., Bock, E., Cox, J.C., Langworthy, T.A., and White, D.C. (1986) Signature fatty acids in the polar lipids of acid-producing *Thiobacillus* spp.: methoxy, cyclopropyl, alpha-hydroxy-cyclopropyl and branched and normal monoenoic fatty acids. *FEMS Microbiol. Ecol.* 38, 67–77.

Kohring, L.L., Ringelberg, D.B., Devereux, R., Stahl, D.A., Mittelman, M.W., and White, D.C. (1994) Comparison of phylogenetic relationships based on phospholipid fatty acid profiles and ribosomal RNA sequence similarities among dissimilatory sulfate-reducing bacteria. *FEMS Microbiol. Lett.* 119, 303–308.

Lambert, G.R. and Smith, G.D. (1980) The hydrogen metabolism of cyanobacteria (blue-green algae). *Biol. Rev. Cambridge Philos. Soc.* 56, 589–660.

Li, Y. and Gregory, S. (1974) Diffusion of ions in sea water and in deep-sea sediments. *Geochim. Cosmochim. Acta* 38, 703–714.

López-Cortés, A. (1990) Microbial mats in tidal channels at San Carlos, Baja California, Sur, Mexico. *Geomicrobiol. J.* 8, 69–85.

Nübel, U., Garcia-Pichel, F., and Muyzer, G. (1997) PCR primers to amplify 16S rRNA genes from cyanobacteria. *Appl. Environ. Microbiol.* 63, 3327–3332.

Nübel, U., Bateson, M.M., Madigan, M.T., Kühl, M., and Ward, D.M. (2001) Diversity and distribution in hypersaline mats of Bacteria related to *Chloroflexus* spp. *Appl. Environ. Microbiol.* 67, 4365–4371.

Oren, A., Padan, E., and Malkin, S. (1979) Sulfide inhibition of photosystem II in cyanobacteria (blue green algae) and tobacco chloroplasts. *Biochim. Biophys. Acta* 546, 270–279.

Ploug, H., Prufert-Bebout, L., and Jørgensen, B.B. (1998) Photosynthetic adaptations to spectral scalar irradiance among cyanobacteria within a stratified microbial mat community. In *Environmental Controls on Cyanobacterial Distribution: The Role of Irradiance* [Ph.D. Dissertation], University of Århus, Århus, Denmark.

Potts, M., Olie, J.J., Nickels, J.S., Parsons, J., and White, D.C. (1987) Variation in phospholipid ester-linked fatty acids and carotenoids of dessicated *Nostoc commune* (Cyanobacteria) from different geographic locations. *Appl. Environ. Microbiol.* 53, 4–9.

Prufert-Bebout, L., Ploug, H., Garcia-Pichel, F., and Kühl, M. (1998) Adaptations of *Microcoleus chthonoplastes* to benthic light fields as studied *in situ* by microsensors. In *Environmental Controls on Cyanobacterial Distribution: The Role of Irradiance* [Ph.D. Dissertation], University of Århus, Århus, Denmark.

Reeburgh, W.S. (1980) Anaerobic methane oxidation: rate depth distributions in Skan Bay sediments. *Earth Planet. Sci. Lett.* 47, 345–352.

Reid, R.P., Visscher, P.T., Decho, A.W., Stolz, J.F., Bebout, B.M., Dupraz, C., Macintyre, I.G., Pinckney, J., Paerl, H.W., Prufert-Bebout, L., Steppe, T.F., and Des Marais, D.J. (2000) The role of microbes in accretion, lamination and lithification in modern marine stromatolites. *Nature* 406, 989–992.

Revsbech, N.P. and Jørgensen, B.B. (1986) Microelectrodes: their use in microbial ecology. *Adv. Microb. Ecol.* 9, 293–352.

Revsbech, N.P., Jørgensen, B.B., Blackburn, T.H., and Cohen, Y. (1983) Microelectrode studies of the photosynthesis and $O_2$, $H_2S$, and pH profiles of a microbial mat. *Limnol. Oceanogr.* 28, 1062–1074.

Schidlowski, M. (1988) A 3,800-year-old isotopic record of life from carbon in sedimentary rocks. *Nature* 333, 313–318.

Sherwood, J.E., Stagnitti, F., Kokkinn, M.J., and Williams, W.D. (1991) Dissolved oxygen concentrations in hypersaline waters. *Limnol. Oceanogr.* 36, 235–250.

Visscher, P.T. and Kiene, R.P. (1994) Production and consumption of volatile organosulfur compounds in microbial mats. In *Microbial Mats: Structure, Development and Environmental Significance*, edited by L.J. Stal and P. Caumette, Springer-Verlag, New York, pp. 279–284.

Visscher, P.T. and Van Gemerden, H. (1991) Production and consumption of dimethylsulfoniopropionate in marine microbial mats. *Appl. Environ. Microbiol.* 57, 3237–3242.

Volkman, J.K. (1986) A review of sterol markers for marine and terrigenous organic matter. *Org. Geochem.* 9, 83–99.

Walter, M.R. (1976) *Stromatolites*, Elsevier Scientific, Amsterdam.

Ward, D.M., Brassell, S.C., and Eglinton, G. (1985) Archaebacterial lipids in hot-spring microbial mats. *Nature* 318, 656–659.

Ward, D.M., Weller, R., and Bateson, M.M. (1990) 16S rRNA sequences reveal numerous uncultured microorganisms in a natural community. *Nature* 345, 63–65.

Wieland, A., de Beer, D., Damgaard, L.R., Khl, M., van Dusschoten, D., and Van As, H. (2001) Fine-scale measurement of diffusivity in a microbial mat with nuclear magnetic resonance imaging. *Limnol. Oceanogr.* 46, 248–259.

Wilson, M.V. and Botkin, D.B. (1990) Models of simple microcosms: emergent properties and the effect of complexity on stability. *Am. Nat.* 135, 414–434.

Address reprint requests to:
*Dr. Brad M. Bebout*
*NASA Ames Research Center*
*Mail Stop 239-4*
*Moffett Field, CA 94035-1000*

*E-mail:* Brad.M.Bebout@nasa.gov